Performance Evaluation of Event-Triggered Model Predictive Control for Boost Converter

Ranya Badawi
Department of Electrical and Computer Engineering
Oakland University
Rochester, MI 48309 USA
ranyabadawi@oakland.edu

Jun Chen*
Department of Electrical and Computer Engineering
Oakland University
Rochester, MI 48309 USA
junchen@oakland.edu

***Abstract*—This paper evaluates the performance of an event-triggered model predictive control (MPC) for a DC-DC boost converter. Event-triggered MPC is used to enhance the computational performance of an enumeration-based MPC controlled boost converter by triggering the optimal control problem (OCP) only when an event is triggered as opposed to solving the OCP at every time step. Accordingly, the event-trigger threshold significantly impacts the number of times the OCP is solved. This paper numerically investigates such impact by evaluating various threshold values. The results of this study provide a general guidance to the selection of the threshold value to meet specific system criteria, e.g., balance between computation performance and control performance.**

***Index Terms*—Model Predictive Control, MPC, event-trigger control, optimization control problem, OCP, boost converter**

I. Introduction

Boost converters are used to step up the voltage of an input source to power loads at a higher voltage. They are widely found in battery powered and photovoltaic-cell applications. Power converter control aims to maintain a set voltage despite fluctuations in the source voltage and/or load current. Converter control has been studied extensively and includes both analog and digital control methods [1], [2], where digital control offers several advantages over analog control such as higher accuracy, flexibility, and lower cost [3]. Recent microprocessor advancements such as increased speed and computational capability have enabled the widespread use of digital control, and in particular, model predictive control (MPC). MPC simplifies the controller design and tuning since system objectives and constraints are included in the controller's design phase. [4].

MPC for power converter control has been researched and implemented successfully in numerous studies, [4]–[7]. The MPC controller generally consists of three main parts: a model of the plant being controlled, an optimization control problem (OCP) in the form of constrained optimization, and a receding prediction horizon [8]. In the case of a power converter, the main objective of the controller is to regulate output voltage to track a reference voltage. Additional objectives such as reducing the amount of switching and limiting inductor current can also be added to the cost function.

Due to the finiteness of the potential control actions, an enumerated-based MPC controller can be formulated for boost converters, where an enumerated list of control sequences are constructed as candidate solutions. It then solves the OCP by enumerating the list and selecting the control sequence that minimizes the cost function. Receding horizon policy states that the first element of the optimal sequence is applied to the actuator while the remaining elements of the sequence are discarded [4]. In time-triggered control, the optimization process is repeated at each time sample. The challenge with using MPC for converter control is that the microcontroller must have significant computational power as it must solve the optimization problem for all switching sequences within the time sample period. Switching power converters have switching frequencies in the order of tens and hundreds of kHz to reduce the physical size of the passive components (i.e., inductors and capacitors). The time sample period must be at least one-half $(1/2)$ the target switching period. An additional challenge is introduced due to the non-minimum phase behavior of boost converters which necessitates a longer prediction horizon [5], [9].

To address MPC's computational challenge, event-triggered MPC was studied in [10]–[13] to reduce the computational load. In event-triggered MPC, the optimization process is repeated only when an event is triggered; otherwise the previously optimized control sequence is reused without solving a new OCP. Event-triggered MPC for boost converters was first investigated in [10], where the initial simulation results demonstrated a saving in controller computations by up to 93% while achieving comparable performance to time-triggered MPC. However, the selection of threshold value, a key design parameter in event-triggered MPC, was not investigated in [10]. In this paper, we address this by evaluating the performance of the converter with different event-trigger thresholds through simulation. The reported findings will provide a general guidance on how to select the trigger threshold to achieve specific converter criteria such as computation requirements, voltage regulation, reduced voltage ripple and response time.

The rest of this paper is organized as follows. Section II gives an overview of the discrete-time model of the DC-DC

This work is supported in part by SECS Faculty Startup Fund and URC Faculty Research Fellowship at Oakland University.

*Jun Chen is the corresponding author.

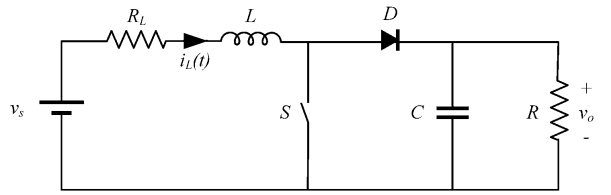

Fig. 1. DC-DC Boost Converter

boost converter. Section III explains time-triggered and event-triggered enumeration-based MPC. Simulation results highlighting the performance of event-triggered MPC are presented and discussed in Section IV, and the paper is concluded in Section V.

II. BOOST CONVERTER DISCRETE-TIME MODEL

The first step to creating an MPC controller is to develop an accurate model of the controlled system, i.e, the boost converter. We briefly introduce the model and refer the reader to [5] and [10] for details.

The circuit diagram of the boost converter is shown in Fig. 1. A boost converter steps up the input voltage by actuating switch S. When switch S is ON (i.e., closed) energy is stored in the inductor as the current through the inductor increases. When switch S is OFF (i.e., open), the current through the inductor decreases and the stored energy is released to the load. If the inductor current is greater than zero throughout the converter's operation, the converter is said to operate in continuous conduction mode (CCM). If the inductor current reaches zero during operation, then the converter is said to operate in discontinuous conduction mode (DCM). The mathematical model developed for the MPC controller captures both CCM and DCM operating modes.

The discrete-time model is derived using the continuous-time model of the boost converter detailed in [5], [10]. The forward Euler approximation is applied where T_s is defined as the time step. The state variable matrix $x[k]$ is defined in (1), where $i_L[k]$ is the inductor current and $v_o[k]$ is the output voltage.

$$x[k] = \begin{bmatrix} i_L[k] & v_o[k] \end{bmatrix}^T \tag{1}$$

The converter can operate in any of four different operating states, depending on the shape of the inductor current [5]:

1) Mode 1 represents the converter when switch S is ON and the inductor current is increasing. In this mode, the inductor, L, is connected across the input source while the capacitor is sourcing current to the load.
2) Mode 2 is when switch S is OFF and the inductor current is decreasing and is positive. Diode D is forward biased and energy stored in the inductor is released to the load.
3) Mode 4 is when both switch S and diode D are OFF and the inductor current is 0. The circuit is reduced to the output capacitor, C, sourcing energy to the load R.
4) Mode 3 is the time average of Modes 2 and 4. It includes the moment when the inductor current decreases from a positive value and reaches 0, defined as τ_1.

The discrete-time state space matrices for all four modes are included below (2). v_s is the source voltage, R_L is the DC resistance of the inductor coil, and the other parameters were declared in the preceding description.

Mode 1:

$$x[k+1] = \begin{bmatrix} 1 - \frac{R_L T_s}{L} & 0 \\ 0 & 1 - \frac{T_s}{RC} \end{bmatrix} x[k] + \begin{bmatrix} \frac{T_s}{L} \\ 0 \end{bmatrix} v_s[k] \tag{2a}$$

Mode 2:

$$x[k+1] = \begin{bmatrix} 1 - \frac{R_L T_s}{L} & -\frac{T_s}{L} \\ \frac{T_s}{C} & 1 - \frac{T_s}{RC} \end{bmatrix} x[k] + \begin{bmatrix} \frac{T_s}{L} \\ 0 \end{bmatrix} v_s[k] \tag{2b}$$

Mode 3:

$$x[k+1] = \begin{bmatrix} 1 - \frac{R_L \tau_1}{L} & -\frac{\tau_1}{L} \\ \frac{\tau_1}{C} & 1 - \frac{T_s}{RC} \end{bmatrix} x[k] + \begin{bmatrix} \frac{\tau_1}{L} \\ 0 \end{bmatrix} v_s[k] \tag{2c}$$

Mode 4:

$$x[k+1] = \begin{bmatrix} 1 & 0 \\ 0 & 1 - \frac{T_s}{RC} \end{bmatrix} x[k] \tag{2d}$$

III. MODEL PREDICTIVE CONTROL

We will briefly discuss time-triggered MPC followed by the event-triggered MPC proposed in [10].

A. Time-triggered Enumeration-based MPC

We start with the assembly of a full set of switching sequences. The number of elements in the switching sequence is equal to the length of horizon, N. Each switching sequence is in the form $U[k] = [u[k], u[k+1] \dots u[k+N-1]]$, where $u[k]$ is defined as

$$u[k] = \begin{cases} 1 & \text{when switch } S \text{ is closed/ON,} \\ 0 & \text{when switch } S \text{ is open/OFF.} \end{cases} \tag{3}$$

The total number of switching sequences is therefore 2^N. The time duration of the prediction horizon is NT_s with T_s being the sampling time. It was noted earlier that boost converters require longer prediction horizons due to their non-minimum phase behavior, but this would require a significant increase in the prediction horizon length, N. To address this, a move blocking scheme is implemented to extend the duration of the prediction horizon without having to increase N significantly. Details about the move blocking scheme is in [5]. At every time step, the MPC solves an OCP in which the

cost function in (4) is evaluated for each switching sequence. The cost function is formulated as follows.

$$\min_{U_o} \quad \sum_{\ell=k}^{k+N-1} \left(|v_{o,err}[\ell+1|k]| + \lambda|\Delta u[\ell|k]|\right) \tag{4a}$$

$$\text{s.t.} \quad \text{System dynamics } (2) \tag{4b}$$

The MPC controller samples the input voltage, inductor current and output voltage and calculates the projected output voltage, inductor current and evaluates the cost function (4) for each of the predefined switching sequences $U[k]$. Two objectives of the control action are captured in the cost function: 1) track the reference voltage and 2) reduce the switching frequency. The first term in the cost function captures the first objective, where the absolute voltage error is calculated using $(v_{o,err}[k] = v_{ref} - v_o[k])$. To reduce the amount of switching, the difference in switch state $(\Delta u[k] = u[k] - u[k-1])$ is also captured. A weighing factor, λ, is applied to the switch state difference and is adjusted depending on how much it is desired to penalize this difference. The switching sequence which minimizes the cost function value in (4) is then selected as the optimal switching sequence $U_o[k]$. The first element of the sequence is then applied to the switch, S. For time-triggered MPC, this procedure is repeated at every time-step for all 2^N switching sequences.

B. Event-Triggered Enumeration-based MPC

The enumeration technique evaluates the objective function for all switching sequences at every time-step which requires the controller to operate for extensive periods of time during all operating modes. Increasing the prediction horizon also demands higher computational power as the number of switching sequences increases exponentially. This eventually leads to significant energy dissipation by the controller. To address this issue, event-triggered MPC was proposed to solve the optimization problem only when an event is triggered. A brief description is given below. For more details, the reader is to refer to [10].

At time t, the event-triggered MPC block outputs the entire optimal switching sequence U_t, optimal state trajectory X_t, and the current switching signal u. An additional output, index k, points to the element in U_t that was last accessed to actuate switch S. These outputs are all fed back to the MPC block as inputs after one time step delay. The system proposed in [10] is displayed in Fig.2. Specifically, an event e is defined by:

$$e = \begin{cases} 1 & \text{if } ||X_{t_1}(2,k) - v_o|| > \delta \text{ or } k > k_{max}, \\ 0 & \text{Otherwise.} \end{cases} \tag{5}$$

During initial operation, the event-triggered MPC controller samples the state variables i_L and v_o and solves the OCP for all switching sequences, then finds the optimal switching sequence, U_t, where $U_t = U_o$. The switch is actuated using the first element in U_t (i.e., $u = U_t(1)$). U_t, X_t and u are passed to the output along with index k which is set initially to 0. Upon the next time step, the information calculated from this initial step can then be used for event-trigger control. Again,

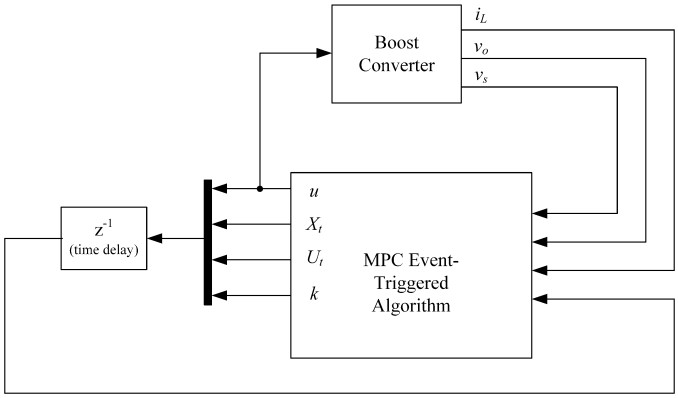

Fig. 2. DC-DC Boost Converter with Event-Triggered MPC Control [10]

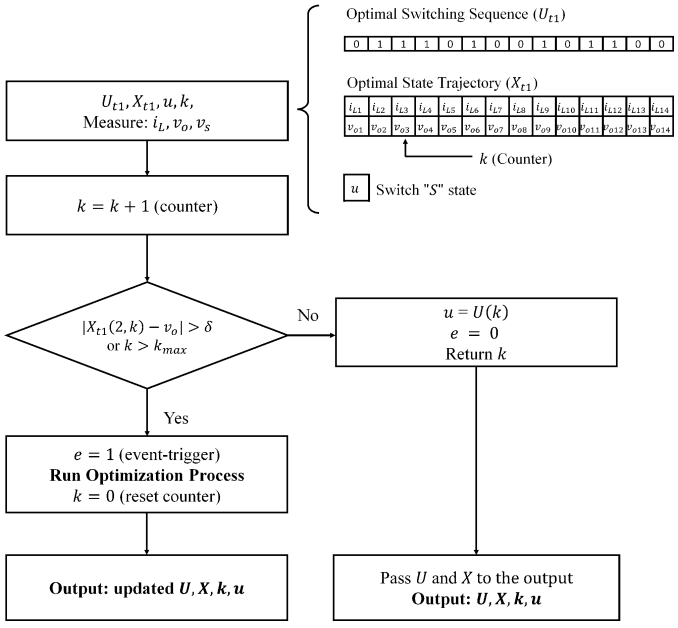

Fig. 3. Event-Triggered MPC Control Flow Chart

the state variable $x[k]$ is sampled at this time step, index k is incremented, and e is then evaluated using (5), where the measured voltage, v_o, or, $x(2)$ is compared to $X_{t_1}(2,k)$. $X_{t_1}(2,k)$ is the predicted output voltage in the optimal state trajectory calculated from the previous step at index k. If the absolute difference between the measured voltage and the projected output voltage exceeds the trigger threshold δ, e is set to 1, and an event is triggered. When triggered, the enumeration based MPC solves the optimization problem and generates a new optimal control sequence, state trajectory and switch state. Otherwise, when $e = 0$, the control action is determined using the next switch state in the optimal sequence, U_{t_1}, computed at the last event, thus avoiding running the optimization problem for the 2^N switching sequences. Fig. 3 outlines the flowchart of the proposed event-triggered MPC control algorithm.

The selection of the event-trigger threshold, δ, significantly

TABLE I
SIMULATION PARAMETERS

Converter and Controller Parameter	Value
Inductor (L)	$550\mu H$
Inductor DC Resistance (R_L)	1.3Ω
Output Capacitance (C)	$220\mu F$
Load Resistance (R)	73Ω
Sampling Period (T_s)	$5\mu s$
Prediction Horizon (N), k_{max}	14
N_1	1
Move Blocking Coefficient (n_s)	4
Weight in Objective Function Lambda (λ)	0.5

impacts the performance of the converter. To assess this impact, we implement the closed loop system consisting of the boost converter and MPC controller in MATLAB/Simulink and evaluate converter performance using different values of δ. The simulation results are discussed and reported in the following section.

IV. SIMULATION RESULTS

The performance of event-trigger MPC control on the boost converter is evaluated during startup, step change in input voltage and step changes in voltage reference with different values of trigger threshold δ. The parameters used in all simulations are listed in Table I. Throughout our investigation, we plot the averaged event frequency using a moving window to indicate computational savings.

A. Event-Trigger Threshold Impact on Start-up Time

Different start-up conditions were simulated in which the event-trigger threshold of the MPC controller was varied. In all cases, the controller kept switch S open initially during start-up to charge the output capacitor to the input voltage which caused an initial inrush of current. Once the output capacitor was charged to the input voltage, the controller began to actuate the switch, and the converter boost the voltage to the voltage setpoint (v_{ref}). It was observed that the desired reference is reached at about the same time for both time and event-triggered MPC implementations for most operating conditions. Start-up time was mostly independent of our selection of the event-trigger threshold δ value. However, start-up time was dependent on operating conditions with the results tabulated in Table II. Simulated waveforms for different trigger thresholds for the operating case: $v_s = 10V$ and $v_{ref} = 20V$ are shown in Fig. 4.

B. Event-Trigger Threshold Impact on Steady-state Operation

With event-triggered MPC, once the converter reaches steady-state, the number of event triggers is significantly decreased. Event frequency for different steady state operating

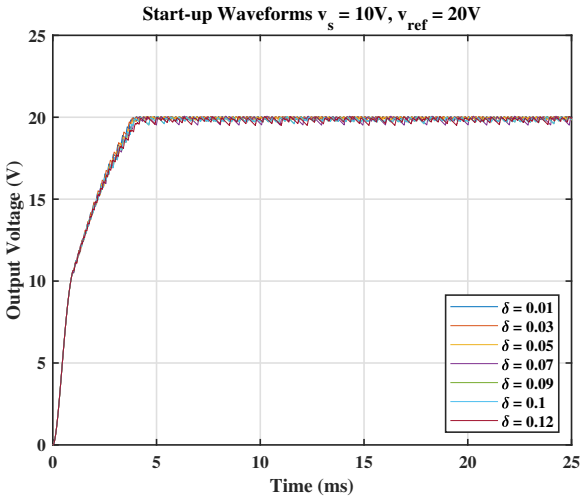

Fig. 4. Start-up (v_s = 10V and v_{ref} = 20V)

TABLE II
START-UP TIME SUMMARY

Operating Conditions	Time-triggered MPC	Event-triggered MPC
$v_s = 10V$, $v_o = 15V$	$2.2ms$	$2.2ms$
$v_s = 10V$, $v_o = 20V$	$3.9ms$	$4.3ms$
$v_s = 10V$, $v_o = 30V$	$13.2ms$	$16ms$
$v_s = 15V$, $v_o = 20V$	$1.6ms$	$1.6ms$
$v_s = 15V$, $v_o = 30V$	$3.9ms$	$3.9ms$

conditions, in addition to the tracking error were tabulated in Table III, where tracking error was calculated by

$$T.E. = \sqrt{\frac{\sum_{i=1}^{n}(v_o[i] - v_{ref}[i])^2}{n}}. \quad (6)$$

The results reported in Table III show that increasing the trigger threshold δ significantly reduces the computation burden of the controller during steady state operation but increases the tracking error. Increasing δ also increases the output voltage ripple and peak inductor current. It was noted (Fig. 5) that the converter was not able to reach the reference voltage when $v_s = 10V$ and $v_{ref} = 30V$ for $\delta \geq 0.09$. Additionally, during steady-state operation the converter experienced irregularities in the output waveform when $v_s = 10V$ and $v_{ref} = 15V$ for $\delta \geq 0.1$.

C. Event-Trigger Threshold Impact on Step Changes in the Output Reference Voltage

The performance of the converter with different trigger thresholds was evaluated when the output reference voltage was stepped up from 15V to 30V. As can be seen from Fig. 6, the output achieves a regulated 30V output at approximately 19ms for time-triggered MPC. The performance of the converter with different trigger thresholds was evaluated when the output reference voltage was stepped up at $7.5ms$ from 15V

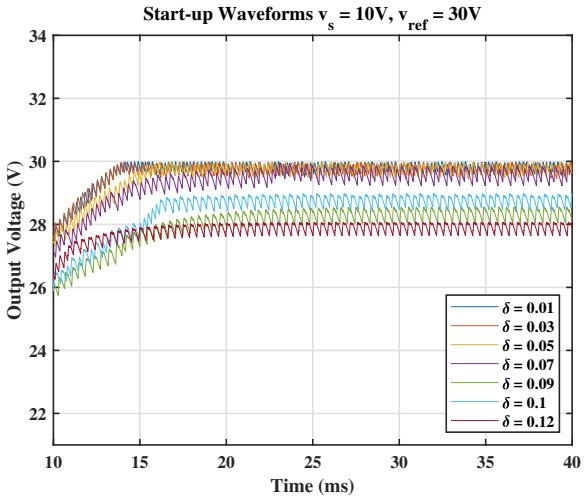

Fig. 5. Start-up and steady-state operation (v_s = 10V and v_{ref} = 30V)

TABLE III
EVENT-TRIGGER IMPACT ON STEADY-STATE OPERATION - RESULTS SUMMARY

Event Frequency:		
Steady-State Conditions	$\delta = 0.01$	$\delta = 0.07$
$v_s = 10V$, $v_o = 15V$	30%	2.7%
$v_s = 10V$, $v_o = 20V$	33%	7%
$v_s = 10V$, $v_o = 30V$	42%	11%
$v_s = 15V$, $v_o = 30V$	44%	12%
Tracking Error [V]:		
Steady-State Conditions	$\delta = 0.01$	$\delta = 0.07$
$v_s = 10V$, $v_o = 15V$	0.024	0.09
$v_s = 10V$, $v_o = 20V$	0.049	0.178
$v_s = 10V$, $v_o = 30V$	0.216	0.42
$v_s = 15V$, $v_o = 30V$	0.072	0.1
Output Voltage Ripple [Vpp]:		
Steady-State Conditions	$\delta = 0.01$	$\delta = 0.07$
$v_s = 10V$, $v_o = 15V$	0.095	0.36
$v_s = 10V$, $v_o = 20V$	0.163	0.54
$v_s = 10V$, $v_o = 30V$	0.43	0.62
$v_s = 15V$, $v_o = 30V$	0.236	0.377

to 30V, where $v_s = 10V$. As can be seen from Fig. 7, the converter achieves a regulated $30V$ output at approximately $19ms$ when $\delta = 0.01$ and at $23.5ms$ when $\delta = 0.07$. The event frequency increases as well as the inductor current during the step up in reference voltage. Once the converter reaches regulation, the inductor current is reduced. Results are summarized in Table IV.

Next, the output voltage reference is changed from $20V$ to $15V$ at $7.5ms$ for $\delta = 0.01$ and 0.07 with waveforms plotted in Fig. 8. During the step down in reference voltage,

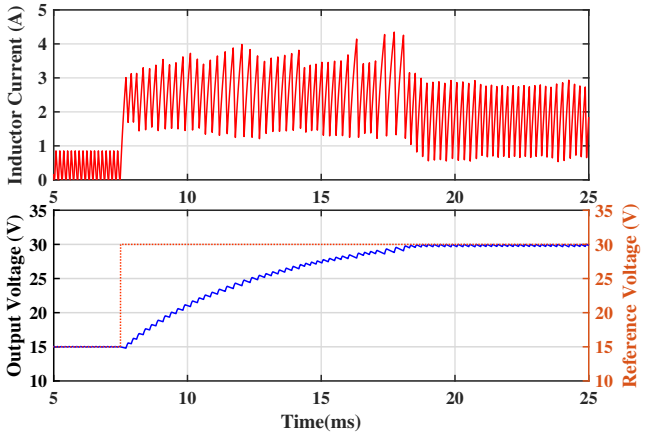

Fig. 6. Reference step-up from 15V to 30V (Time-triggered MPC) [10]

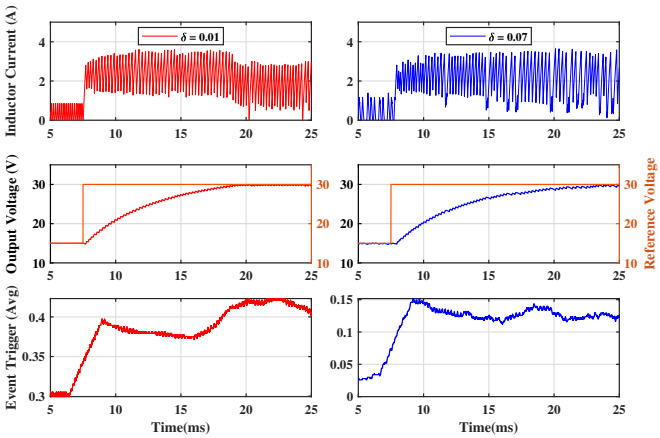

Fig. 7. Reference voltage step-up from 15V to 30V (Event-Triggered MPC)

switch S is OFF and the inductor current goes to zero allowing the capacitor to discharge into the load to reduce the output voltage. A subset of the results for different thresholds is summarized in Table IV.

TABLE IV
VOLTAGE REFERENCE CONVERTER RESPONSE FOR DIFFERENT EVENT THRESHOLDS

	$\delta = 0.01$	$\delta = 0.05$	$\delta = 0.07$
$v_{ref} = 15V \rightarrow 30V$, $v_s = 10V$			
Transient time [ms]	11.5	14	16
Event Frequency	42.5%	19.5%	15%
$v_{ref} = 20V \rightarrow 15V$, $v_s = 10V$			
Transient time [ms]	4.6	4.6	4.6
Event Frequency	28%	7.5%	2.5%

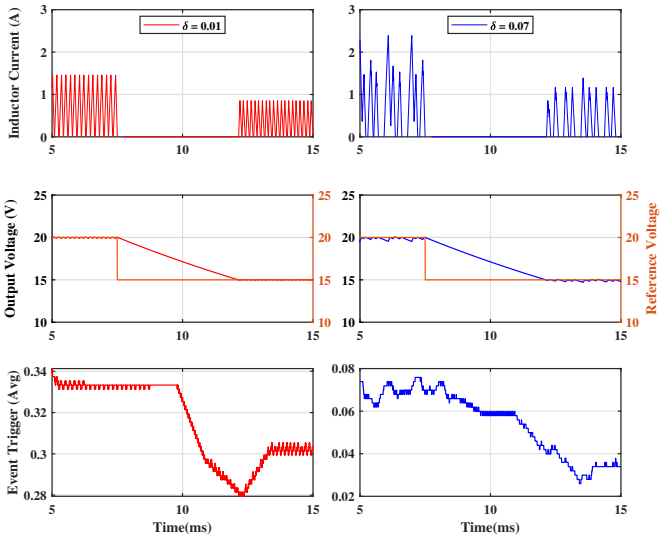

Fig. 8. Reference voltage step-down from 20V to 15V (Event-Triggered MPC)

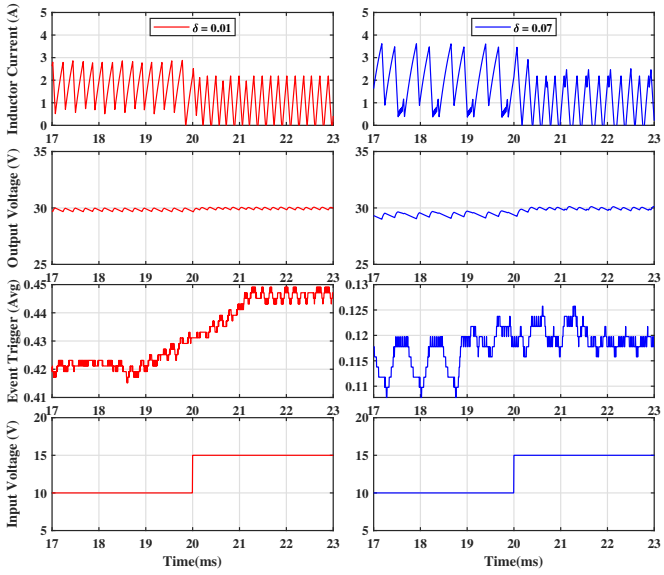

Fig. 9. Input voltage step-up from 10V to 15V (Event-triggered MPC)

D. Event-Trigger Threshold Impact on Step Change in the Input Voltage

A step change in the input voltage from $10V$ to $15V$ at $20ms$ after steady state operation with v_{ref} set to $30V$ was simulated. The line transient response of the converter for $\delta = 0.01$ and $\delta = 0.07$ are displayed in Fig. 9. In both cases, event trigger frequency increases as the input voltage increases. The event frequency during the transient increases by 2% when $\delta = 0.01$, where as it only increases by 0.5% when $\delta = 0.07$. The output voltage remains almost undisturbed during the input transient as the response of the controller is almost immediate.

V. CONCLUSION

This paper explores the impact of the event-trigger threshold, δ, on the performance of an event-triggered model predictive control (MPC) for a DC-DC boost converter, supplementing our prior work where an event-triggered enumeration-based MPC was proposed to reduce the computation burden of a time-triggered MPC controller. Simulation results demonstrate the impact of event-trigger threshold on the performance of the converter during different operating conditions. Generally, increasing the threshold trigger reduces the number of computations performed but increases the tracking error and voltage ripple during steady state operation. A trade-off must be made between the number of computations and meeting specific performance targets. Future research directions include (1) implementation of the proposed controller in hardware to verify the feasibility of real-time implementation and (2) applications to battery and renewable energy control [14], [15].

REFERENCES

[1] S. Kouro, P. Cortés, R. Vargas, U. Ammann, and J. Rodríguez, "Model predictive control—a simple and powerful method to control power converters," *IEEE Transactions on Industrial Electronics*, vol. 56, no. 6, pp. 1826–1838, 2008.

[2] M. Saoudi, A. El-Sayed, and H. Metwally, "Design and implementation of closed-loop control system for buck converter using different techniques," *IEEE Aerospace and Electronic Systems Magazine*, vol. 32, no. 3, pp. 30–39, 2017.

[3] M. S. Fadali and A. Visioli, *Digital control engineering: analysis and design*. Academic Press, 2013.

[4] P. P. Karamanakos, "Model predictive control strategies for power electronics converters and ac drives," 2013.

[5] P. Karamanakos, T. Geyer, and S. Manias, "Direct voltage control of dc–dc boost converters using enumeration-based model predictive control," *IEEE Trans. Power Electronics*, vol. 29, no. 2, pp. 968–978, 2013.

[6] Z. Leng and Q. Liu, "A simple model predictive control for buck converter operating in ccm," in *IEEE PRECEDE*, 2017, pp. 19–24.

[7] T. Geyer, G. Papafotiou, R. Frasca, and M. Morari, "Constrained optimal control of the step-down dc–dc converter," *IEEE transactions on power electronics*, vol. 23, no. 5, pp. 2454–2464, 2008.

[8] J. Chen, M. Liang, and X. Ma, "Probabilistic analysis of electric vehicle energy consumption using MPC speed control and nonlinear battery model," in *2021 IEEE Green Technologies Conference*, Denver, CO, April 7–9, 2021.

[9] F. A. Villarroel, J. R. Espinoza, M. A. Pérez, R. O. Ramírez, C. R. Baier, D. Sbárbaro, J. J. Silva, and M. A. Reyes, "Stable shortest horizon fcs-mpc output voltage control in non-minimum phase boost-type converters based on input-state linearization," *IEEE Transactions on Energy Conversion*, vol. 36, no. 2, pp. 1378–1391, 2021.

[10] R. Badawi and J. Chen, "Enhancing enumeration-based model predictive control for dc-dc boost converter with event-triggered control," in *European Control Conference*, London, UK, July 12–15, 2022.

[11] J. Chen, X. Meng, and Z. Li, "Reinforcement learning-based event-triggered model predictive control for autonomous vehicle path following," in *American Control Conference*, Atlanta, GA, June 8–10, 2022.

[12] J. Chen and Z. Yi, "Comparison of event-triggered model predictive control for autonomous vehicle path tracking," in *IEEE Conf. Control Technology and Applications*, San Diego, CA, Aug. 8–11, 2021.

[13] S. Huang and J. Chen, "Event-triggered model predictive control for autonomous vehicle with rear steering," *SAE Technical Paper*, no. 2022-01-0877, 2022.

[14] J. Chen, A. Behal, and C. Li, "Active cell balancing by model predictive control for real time range extension," in *2021 IEEE Conference on Decision and Control*, Austin, TX, USA, December 13–15, 2021.

[15] J. Chen, Z. Li, and X. Yin, "Optimization of energy storage size and operation for renewable-ev hybrid energy systems," in *2021 IEEE Green Technologies Conference*, Denver, CO, April 7–9, 2021.